Available online at www.sciencedirect.com
SCIENCE DIRECT®
Journal of Solid State Chemistry 179 (2006) 33–40
JOURNAL OF SOLID STATE CHEMISTRY
www.elsevier.com/locate/jssc

Visible light photoelectrochemical activity of $K_4Nb_6O_{17}$ intercalated with photoactive complexes by electrostatic self-assembly deposition

Ugur Unal*, Yasumichi Matsumoto, Naoko Tamoto, Michio Koinuma, Masato Machida, Kazuyoshi Izawa

Faculty of Engineering, Department of Applied Chemistry, Kumamoto University, Kurokami 2-39-1, Kumamoto 860-8555, Japan

Received 13 July 2005; received in revised form 23 September 2005; accepted 24 September 2005
Available online 25 October 2005

Abstract

Electrostatic self-assembly deposition (ESD) results in the intercalation of $Ru(bpy)_3^{2+}$ or methylene blue (MB) into the niobate layered oxide right after the cations come into contact with $[Nb_6O_{17}]^{4-}$ nanosheets. Monolayers can be obtained by the exfoliation of proton exchanged $K_4Nb_6O_{17}$ (KNbO) in an aqueous tetrabutylammonium (TBA) solution as revealed by the atomic force microscopy micrographs. UV-vis spectra show that intercalated films are able to absorb in the visible light range. Heat-treatment of $Ru(bpy)_3^{2+}$ resulted in the red-shift in the absorption spectra, which was assigned to the enhancement in the interaction between the complex molecules and $[Nb_6O_{17}]^{4-}$ host layer. Intercalated niobate layered oxides are able to produce photocurrent as a result of the electron transfer from the excited guest molecule to the host layer under visible light illumination. $Ru(bpy)_3^{2+}$ intercalated niobate layered oxide shows photocatalytic activity under visible light illumination to produce H_2 from water–methanol solution.

Keywords: Layered oxides; Niobate; Exfoliation; Intercalation; Methylene blue; Photochemistry; Water splitting

1. Introduction

Layered oxide materials have been widely studied in the past couple of decades, because of their unique, highly applicable chemical and physical properties. Preparation, characterization and application of several series of inorganic layered oxides in different fields are of common interest. Among them is $K_4Nb_6O_{17}$ (KNbO) with its unique layered structure. KNbO possesses two alternative interlayer spaces formed by repeating $[Nb_6O_{17}]^{4-}$ layers between which K^+ exist to hold the layers together and to maintain the charge balance. Hydration and ion exchange behavior of these alternative interlayers are different from each other [1]. Introduction of wide range of cations and molecules into the interlayer of KNbO has been carried out on the basis of the ion-exchange principles [2–5] and intercalation of large molecules, such as dyes or $Ru(bpy)_3^{2+}$ complex were accomplished after opening up the interlayer space with alkylammoniums to make the intercalation possible [6–13]. Intercalation or ion-exchange process, however, might take days or weeks, and only partial exchange is obtained. Recently, we have reported electrostatic self-assembly deposition (ESD) technique for the intercalation of several complexes into the layered titanate oxide [14]. The technique provides a quick and reliable way to introduce any complex molecule or a cation into the interlayer of these layered oxides. Intercalation takes place immediately after mixing the solutions of negatively charged titanate nanosheets and complex cations under controlled pH [14].

Photocatalytic and photoluminescent properties of KNbO have been widely studied by many researchers. Domen et al. showed that KNbO, hosting various cations in the interlayer is able to catalyze the photolysis of water efficiently [15–22]. The process, however, takes place under UV light because of the large band-gap of the host oxide. Since the use of visible light in photocatalytic reactions in order to utilize readily available sunlight is important, several modifications have been carried out in the inter-

*Corresponding author. Fax: +81 96 342 3679.
E-mail address: ugurunal@chem.kumamoto-u.ac.jp (U. Unal).

0022-4596/$ - see front matter © 2005 Elsevier Inc. All rights reserved.
doi:10.1016/j.jssc.2005.09.038

layer or on the surface of the photocatalyst to do so. For instance, narrow band-gap semiconductors were introduced into the interlayer and these systems were reported to be able to utilize visible light in photocatalytic reactions [23–25]. In addition, Kim et al. and several other researchers have reported photocatalytic KNbO systems working under visible light in the presence of photoactive dyes or complexes [26–29]. In these systems, an electron is injected into the host layer from the excited photoactive molecules on the surface under visible light. The activity of similar molecules in the interlayer also indicated that electron transfer from the interlayer molecule to the host layer is possible under illumination with visible light. These results were concluded after detailed studies of host–guest interaction with spectral analyses [30–33].

In this work, we have investigated the exfoliation of $[Nb_4O_{17}]^{4-}$ sheets and the intercalation of $Ru(bpy)_3^{2+}$ complex and MB into the interlayer of KNbO by ESD technique. Photoelectrochemical properties of KNbO films deposited by electrophoretic deposition method were previously reported by our laboratory [34]. In current research, photoelectrochemical properties of intercalated compounds were discussed in terms of the interaction between the interlayer molecules and the $[Nb_4O_{17}]^{4-}$ host layer. In addition, photocatalytic activity of $Ru(bpy)_3^{2+}$ intercalated KNbO to release H_2 in water/methanol solution under visible light illumination was reported.

2. Experimental section

Layered potassium niobate ($K_4Nb_6O_{17}$) was prepared by a conventional solid-state method. The mixture of Nb_2O_5 (Wako Pure Chemical, 99.9%) and K_2CO_3 (Wako Pure Chemical, 99.9%) was calcined at 1473 K for 15 min in a Pt crucible [16]. The final product of $K_4Nb_6O_{17}$ powder was pulverized in a mortar to decrease particle size to less than about 10 μm. The $K_4Nb_6O_{17}$ sample was hydrated at this stage ($K_4Nb_6O_{17}\cdot 3H_2O$) according to its XRD pattern. The powder was treated with 0.5 M H_2SO_4 for 24 h in order to protonate the interlayers. The proton exchanged powder was exfoliated by introducing tetrabutylammonium (TBA) or ethylamine (EA) molecules into the interlayer. The reaction was carried out in an aqueous tetra(*n*-butyl) ammonium hydroxide or EA solution for 24 h. Exfoliation occurs as a result of the penetration of large TBA or EA molecules into the interlayer, opening up the interlayer to delaminate the powder into single nanosheets. The subsequent centrifugation of the solution under 2000 rpm for 30 min yielded colloidal suspension of individual $[Nb_6O_{17}]^{4-}$ sheets.

The ESD method was used in the intercalation step [14]. The intercalation of $Ru(bpy)_3^{2+}$ complex ions (Aldrich, Tris (2,2′-bipyridil) dichlororuthenium (II) hexahydrate, 99.95%) or methylene blue (Chroma, Methylene Blue med. Puriss.) into the interlayer was performed by the addition of 20 mL of colloidal TBA exfoliated $[Nb_6O_{17}]^{4-}$ sheets into the aqueous solution of $Ru(bpy)_3^{2+}$ or methylene blue. The concentrations of dye solutions were 1 mM and 0.5 mM, respectively. Prior to the addition, the pH of the exfoliation solution was adjusted to 8 with 0.1 M HCl carefully. The addition resulted in an immediate precipitation consisting of a single phase niobate layered oxides intercalated with the $Ru(bpy)_3^{2+}$ or methylene blue molecules. Precipitation occurs as a result of electrostatic principles governing the deposition with ESD mechanism, where negatively charged $[Nb_6O_{17}]^{4-}$ nanosheets combine with the dye cations. pH adjustment is inevitable in this method, because the initial pH values of each solution is quite far away from each other. The exfoliation solution has a pH of around 12, where pH of the $Ru(bpy)_3^{2+}$ or MB solution is around 6. $[Nb_6O_{17}]^{4-}$ sheets precipitate as HNbO at the pH values lower than 5 as a result of H^+ intercalation into the interlayer instead of a desired cation. In addition, $Ru(bpy)_3^{+}$ or MB might produce hydroxides at pH value of the exfoliation solution. Thus, ESD reaction was carried out in a reasonable pH range, which was chosen as 8 and estimated from the titration curves of both solutions.

The topography of the deposited films was observed by Nanoscope E system Atomic Force Microscopy (AFM). The crystal structure and the orientation were analyzed from XRD patterns (using Cu*K*α radiation, Rigaku RINT-2500VHF) of the thin films deposited simply by applying a number of drops of ESD precipitate on a Pt substrate and drying naturally. The compositions of the deposited films were analyzed with an ICP spectrophotometer (Nippon Jarrel Ash IRIS Advantage) and an X-ray photoelectron spectrometer (XPS, VG Scientific Σ-probe). The ICP analyses were made after dissolving the films in HCl solution. Fourier-transformed infrared spectra (FT-IR Perkin Elmer) of the films were obtained with a KBr technique. An appropriate amount of each sample was mixed with 0.3–0.5 g KBr and pressed into a pellet. The samples were analyzed right after preparing the pellets. UV-vis absorption spectra of the deposited oxides were measured using an UV-vis spectrometer (Jasco V-550). TG–DTA curves were obtained by thermal analysis (Seiko TG/DTA).

All electrochemical experiments were carried out in a conventional three-electrode electrochemical cell with a Pt counter electrode and a saturated Ag/AgCl reference electrode. The working electrode potentials referred to this reference electrode unless otherwise stated in this paper. A 500 W ultra-high pressure Hg lamp was used as the light source to measure the photoelectrochemical properties. Cyclic voltammograms (CV) were measured under a potential sweep rate of 20 mV s^{-1}. 0.1 M K_2SO_4 solution was used as a supporting electrolyte solution with a pH of 6.5. N_2 saturation was made in the electrolytes before the electrochemical measurements.

A quartz cell is used as a reaction chamber to conduct photocatalytic experiments. 0.06 g of $Ru(bpy)_3^{2+}$ intercalated sample, which was heat-treated at 300 °C for 2 h was dispersed in 200 mL of 4 M CH_3OH aqueous solution. The

reaction was carried out under stirring and the system was fed with N_2 prior to the measurement. Xe lamp (300 W) was utilized to irradiate the system, during which the light with a wavelength shorter than 420 nm was cut by a cutoff filter. The rate of H_2 evolution was measured by an online gas chromatograph system (Shimadzu, GC-8A), which was connected to the reaction cell.

3. Results and discussion

3.1. Synthesis

The topographic images of the surface of the exfoliated nanosheets were taken by AFM and are given in Fig. 1a. AFM images are consistent with the preservation of the original crystal structure after the exfoliation. The drawn rectangle shows the surface of a unit cell through *b*-axis and connects the uppermost oxygen atoms, which appear as white dots on the AFM pattern. The $a \times c$ dimensions are in accordance with the unit cell parameters of KNbO. In Fig. 1b, the height profile through the drawn axis on the left image indicates the thickness of an individual nanosheet, which is determined to be around 1 nm for nanosheets exfoliated with TBA. The value is very close to the thickness of a monolayer and almost half of the thickness of a bilayer. The lateral sizes of the exfoliated particles are around 200 nm. Thus, AFM images are clear evidences that exfoliation of the layers was accomplished and TBA can exfoliate proton exchanged niobate to individual $[Nb_6O_{17}]^{4-}$ sheets. Exfoliation occurs when bulky ammine molecules penetrate into the acidic interlayer of proton exchanged form of a layered oxide and extend the interlayer gallery to break up the forces holding the layers together to form single nanosheets [35–37]. Saupe et al. reported that the exfoliation yields bilayers initially, but monolayers can be formed subsequently [35]. On the other hand, ethylamine exfoliates niobate layered oxide to bilayers, probably that of layer II, as it can be seen in Fig. 1b, the right image. The exfoliation in this case is most likely to occur throughout the interlayer I only.

Typical XRD pattern of the KNbO was observed in the hydrated form at room temperature as given in Fig. 2. The layer distance of 9.5 Å corresponds to its hydrated form with three water molecules, $K_4Nb_6O_{17} \cdot 3H_2O$. The proton exchange brought about only a very slight change in the layer distance from 9.5 to 9.6 Å according to the shift in

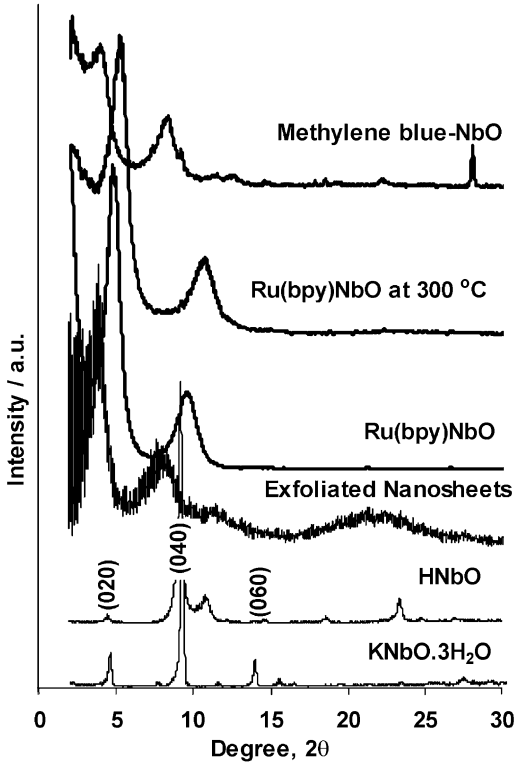

Fig. 2. XRD patterns of $K_4Nb_6O_{17} \cdot 3H_2O$, its proton exchanged form, exfoliated nanosheets, $Ru(bpy)_3^{2+}$ intercalated sample, its heat-treated form at 300 °C and MB intercalated sample, respectively, from bottom to top.

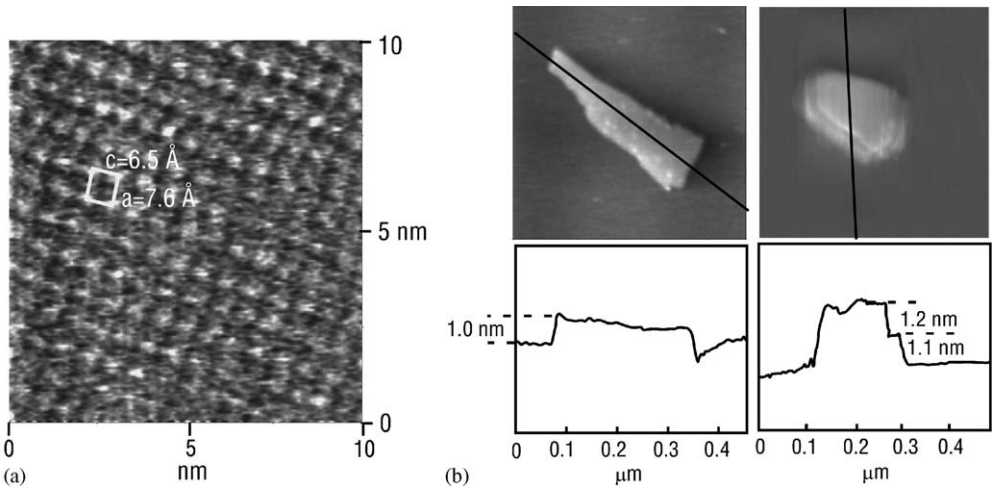

Fig. 1. AFM images of exfoliated $[Nb_6O_{17}]^{4-}$ nanosheets. (a) Atomic resolution image of a $[Nb_6O_{17}]^{4-}$ nanosheet, and (b) nanosheets exfoliated with TBA (left image) and ethylamine (right image).

(040) peak. Protonation is only partial for KNbO and K/Nb ratio is 0.09 after the proton exchange according to the XPS data. The composition of the proton exchanged form is estimated as $K_{0.54}H_{3.46}Nb_6O_{17}$. The film deposited from its exfoliated form by TBA yielded a substantial increase in the layer distance to 22.6 Å, which is in agreement with the result reported by Domen et al. [36]. The corresponding peak in the XRD pattern of the film in Fig. 2 was attributed to the diffraction from the (020) plane, which shows that the TBA exist in the interlayer I only. Both FTIR and XPS data of the film show the presence of TBA molecules in the interlayer. Intercalation of $Ru(bpy)_3^{2+}$ cation and MB into the interlayer by ESD method carried the layer distance to 18.5 Å ($2\theta = 4.78^\circ$) and 21.4 Å ($2\theta = 4.12^\circ$), respectively, as tabulated in Table 1. Layer distances were calculated from the corresponding peaks in the XRD pattern of the films deposited from ESD precipitations.

ESD method is governed by electrostatic principles and interaction between $[Nb_6O_{17}]^{4-}$ layers and $Ru(bpy)_3^{2+}$ or MB molecules brings about a combination between nanosheets and $Ru(bpy)_3^{2+}$ or MB to form intercalated niobate layered oxide after mixing both solutions. Compared to the conventional ion-exchange methods, the advantage of ESD method comes from its rather controllable and quick nature. The intercalation of the molecules takes place immediately as a result of electrostatic interaction forces between oppositely charged species [14]. Taking the size of $Ru(bpy)_3^{2+}$ molecule into consideration, the intercalation of $Ru(bpy)_3^{2+}$ complex occurs in both layers as a result of ESD method. Otherwise, the layer distance of 18.5 Å would be short for niobate layered oxide, hosting $Ru(bpy)_3^{2+}$ only in one layer. The intercalation model is given in Fig. 3a. We can conclude that this intercalation could be B-type [8], thus the corresponding peak is assigned to the diffraction from (040) plane. Similarly, MB is placed in both interlayers with its planar structure and the two possible intercalation models are illustrated in Fig. 3b. If MB molecules lie in the interlayer parallel to $[Nb_6O_{17}]^{4-}$ layers with their long axis, it forms a double layer arrangement when taking the size of the molecule [13] and the interlayer space into consideration. Assuming that it forms a single layer arrangement, the molecule should align in the interlayer slightly inclined to the $[Nb_6O_{17}]^{4-}$ layers with their long axis. Consequently, the corresponding peak can be attributed to (040) diffraction, and the intercalation is B-type, because MB molecules were intercalated into both interlayers. The co-intercalation of proton and/or hydronium ions also occurs to surround the interlayer complex molecules and has an effect on the photoelectrochemical properties, which was also the case for $Ru(bpy)_3^{2+}$ intercalated titanium layered oxides [14]. Heat-treatment resulted in the slight shift of the corresponding peak to higher degrees as a result of the removal of the surrounding water or hydronium ions and enhancement in the photoelectrochemical properties [14]. Similar behavior was observed for $Ru(bpy)_3^{2+}$ intercalated niobate layered oxides as seen in Fig. 2. (040) peak gives the layer distance of 16.6 Å, which is a reasonable value to accommodate $Ru(bpy)_3^{2+}$ in the interlayer without any hydrate.

The chemical compositions of the $Ru(bpy)_3^{2+}$ and MB intercalated niobate layered oxides are given in Table 1. Atomic ratios were calculated on the basis of XPS data and the amount of water was calculated from the TG/DTA data. The chemical composition of the $Ru(bpy)_3^{2+}$ intercalated sample was determined by taking Ru/Nb ratio, which was estimated from the XPS data as 0.05.

Table 1
Chemical compositions and layer distances of the starting and intercalated niobate layered oxides

Chemical composition	Layer distance (Å)
$K_4Nb_6O_{17} \cdot 3H_2O$	9.5
$K_{0.54}H_{3.46}Nb_6O_{17}$	9.6
$K_{0.54}[Ru(bpy)_3]_{0.3}TBA_{0.5}H_{2.66}Nb_6O_{17}$	18.5
$K_{0.54}MB_{0.66}TBA_{0.5}H_{2.3}Nb_6O_{17}$	21.4

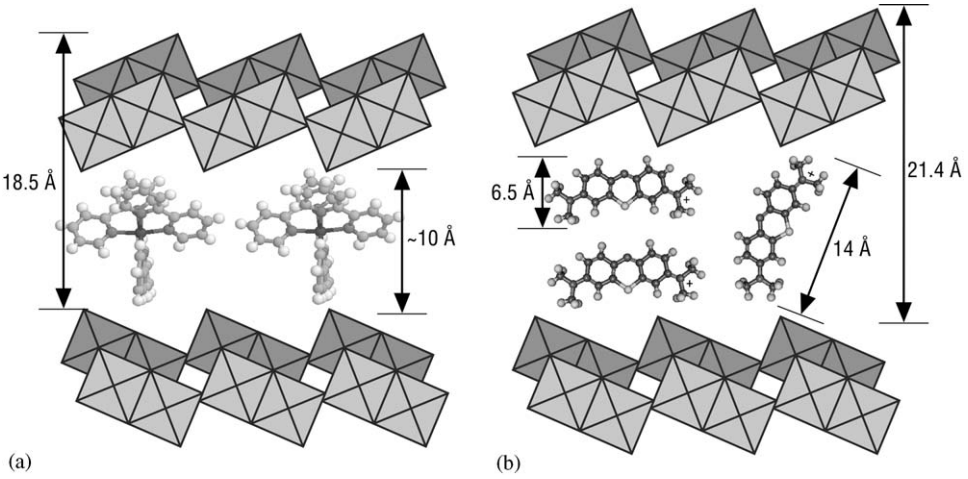

Fig. 3. Intercalation models of: (a) $Ru(bpy)_3^{2+}$ and (b) MB intercalated niobate layered oxides.

$Ru(bpy)_3^{2+}$ molecule is known to occupy an area of 0.84 nm^2 in the interlayer [30] and the charge density of the $[Nb_6O_{17}]^{4-}$ layer is known as 0.126 nm^2 per charge. The theoretical Ru/Nb ratio can be estimated by taking the ratio of a complex cation to the number of Nb atoms in an area that a $Ru(bpy)_3^{2+}$ molecule occupies. Assuming that $Ru(bpy)_3^{2+}$ complex molecules are aligned in the interlayer in a single-layer arrangement and are intercalated into both layers, the maximum $Ru(bpy)_3^{2+}/[Nb_6O_{17}]^{4-}$ ratio would be 0.4 according to the estimation. Consequently, the experimental value indicates that ESD resulted in the occupation of almost all possible sites with $Ru(bpy)_3^{2+}$ molecules and the intercalated molecules were packed densely in the interlayer. On the other hand, $MB/[Nb_6O_{17}]^{4-}$ was estimated as 0.66, which is much larger than the ratio reported by Kaito et al. [13]. These results show that ESD method produces $Ru(bpy)_3^{2+}$ or MB intercalated niobate layered oxides with higher atomic ratios than intercalation compounds obtained by conventional ion-exchange methods [30,32]. XPS and FTIR analyses also revealed that $Ru(bpy)_3^{2+}$ and MB intercalated compounds contains K^+ cations and TBA in the interlayer together with the complexes. Thus, the remaining sites are occupied with TBA, K^+ and protons to maintain the charge balance.

Fig. 4 shows the FTIR spectra of exfoliated and $Ru(bpy)_3^{2+}$ intercalated niobate sheets and its heat-treated form. The FTIR spectrum of exfoliated nanosheets in Fig. 4a shows similar peaks to that of the FTIR spectrum of TBA itself, because TBA molecules coexist in the interlayer. $Ru(bpy)_3^{2+}$ intercalated compound shows a broad OH stretching vibration peak centered at 3400 cm^{-1}, which can be attributed to the hydrogen bonded water. Typical bipyridine bands on the spectrum are also observable in the region of 1400–1600 cm^{-1}. The slight shift of these peaks to lower wavenumbers after the heat-treatment may be attributed to the strain applied on the molecules as a result of the shrinkage in the interlayer space. The peaks due to the C–H stretching bands of TBA at 2870 and 2955 cm^{-1} observed In Fig. 4a and b disappeared after the heat-treatment at 300 °C because of the decomposition and removal of TBA molecules by this temperature as seen in Fig. 4c. The heat-treatment of the $Ru(bpy)_3^{2+}$ intercalated sample does not bring about any other significant change in the FTIR spectra (Figure b and c), because $Ru(bpy)_3^{2+}$ molecules remain intact at 300 °C. As seen in Fig. 5, $Ru(bpy)_3^{2+}$ intercalated niobate layered oxide has three weight loss region on its TGA curve in the range of room T–600 °C. Initially, free or loosely bound water is removed in the room temperature–100 °C region, which is followed by the subsequent removal of interlayer water molecules by 210 °C. Interlayer TBA molecules are also removed in this region. The initiation of the downward curve on the TGA diagram after 300 °C is due to the decomposition of $Ru(bpy)_3^{2+}$ complex molecule in the interlayer, which starts at 320 °C by oxidation. The decomposition and removal of the molecule in the interlayer give rise to an exothermic peak at 400 °C on the DTA curve. $Ru(bpy)_3^{2+}$ intercalated titanate layered oxide also exhibited the same weight loss trend on its TG/DTA diagram [14].

The UV absorption spectra of the exfoliated $[Nb_6O_{17}]^{4-}$ layers and $Ru(bpy)_3^{2+}$ intercalated niobate before and after heat-treatment is given in Fig. 6a–c, respectively. The absorption edge of the niobate around 330 nm is red-shifted to 600 nm and the band is broadened after the intercalation of $Ru(bpy)_3^{2+}$ into the interlayer. Absorption starting at this wavelength is assigned to the metal-to-ligand charge transfer (MLCT) of the $Ru(bpy)_3^{2+}$ molecules in the interlayer. The shift for the intercalated molecules with respect to the peak for its aqueous solution was also reported in other studies related to zeolites [38] or layered materials [8,31,32] and it was assigned to the strained complex molecules [8] and to the chelate-oxide layer and chelate–chelate interaction in the interlayer [32].

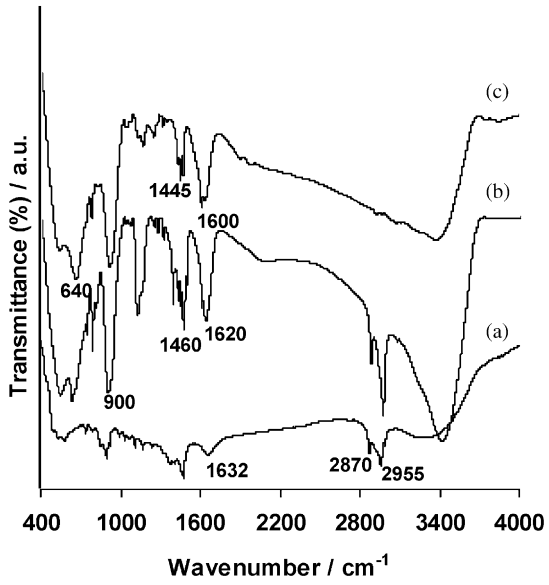

Fig. 4. FTIR spectra of (a) exfoliated nanosheets, and $Ru(bpy)_3^{2+}$ intercalated niobate layered oxide (b) before and (c) after heat-treatment at 300 °C.

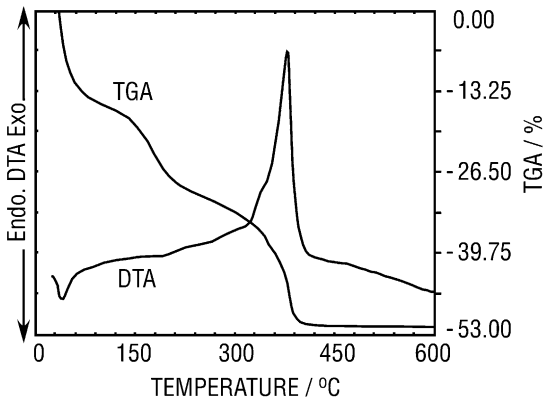

Fig. 5. TG/DTA curves of $Ru(bpy)_3^{2+}$ intercalated niobate layered oxide.

Furthermore, the heat-treatment brought about further red-shift of the absorption edge. $Ru(bpy)_3^{2+}$ intercalated titanate layered oxide also experienced the same behavior of red-shift by heat-treatment [14]. We have assigned the red-shift to the enhancement in the host–guest interaction as a result of the removal of water or hydronium ions surrounding the interlayer complex molecules by heat-treatment at 300 °C. The UV absorption spectrum of MB intercalated sample is also given in Fig. 6d. The very broad absorption band in the visible light region is a result of the presence of MB in the interlayer. The spectrum shows that MB exists as a dimmer, higher aggregate and monomer according to bands around 600 and 500 nm [13,39].

3.2. Photoelectrochemical properties

$Ru(bpy)_3^{2+}$ intercalated film was heat-treated at 300 °C prior to the measurement, because the heat-treated sample had a better response in the visible light range as seen on its UV-vis spectra in Fig. 6. In addition, the heat-treated sample was more stable in the interlayer after the heat-treatment [14]. MB intercalated film was measured without any treatment because of the decomposition of the molecule even at low temperatures. Thus, MB molecules in the interlayer are more likely to deintercalate into the electrolyte during photoelectrochemical measurements as a result of weaker interaction with the host layer and less stability in the interlayer. The cyclic voltammetry measurements of the intercalated niobate layered oxide films were started immediately after the sample was immersed into the N_2 pre-saturated electrolyte to ensure that the interlayer complex molecules do not deintercalate into the electrolyte during the initial stages of the measurement. The cyclic voltammograms of $Ru(bpy)_3^{2+}$ and MB intercalated niobate layered oxide films are given in Fig. 7a and b, respectively. Cyclic voltammograms were measured in 0.1 M K_2SO_4 solution. Illumination of the system was carried out by blocking the path of the light periodically to observe photocurrent. Films produced both anodic and cathodic photocurrents under visible light illumination in which the light with a wavelength shorter than 420 nm was cut by a cutoff filter. The visible photoresponse is in harmony with the result obtained by the UV-vis spectra in Fig. 6. The maximum current density was estimated as 4 and 8 μA/cm^2 for $Ru(bpy)_3^{2+}$ and MB intercalated films, respectively. Higher current density for MB intercalated film might be attributed to a large amount of MB in the interlayer of niobate layered oxide. Under visible light illumination, $Ru(bpy)_3^{2+}$ molecule in the interlayer is excited to its MLCT state to form $Ru(bpy)_3^{2+*}$ by absorbing the visible light, which leads to the photocurrent. The possible electron transfer mechanism is illustrated in

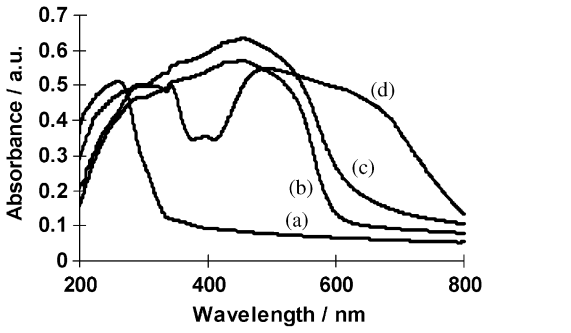

Fig. 6. UV-vis absorbance spectra of the films deposited from (a) exfoliated niobate nanosheets, and $Ru(bpy)_3^{2+}$ intercalated niobate layered oxide (b) before and (c) after heat-treatment at 300 °C, and (d) MB intercalated niobate layered oxide.

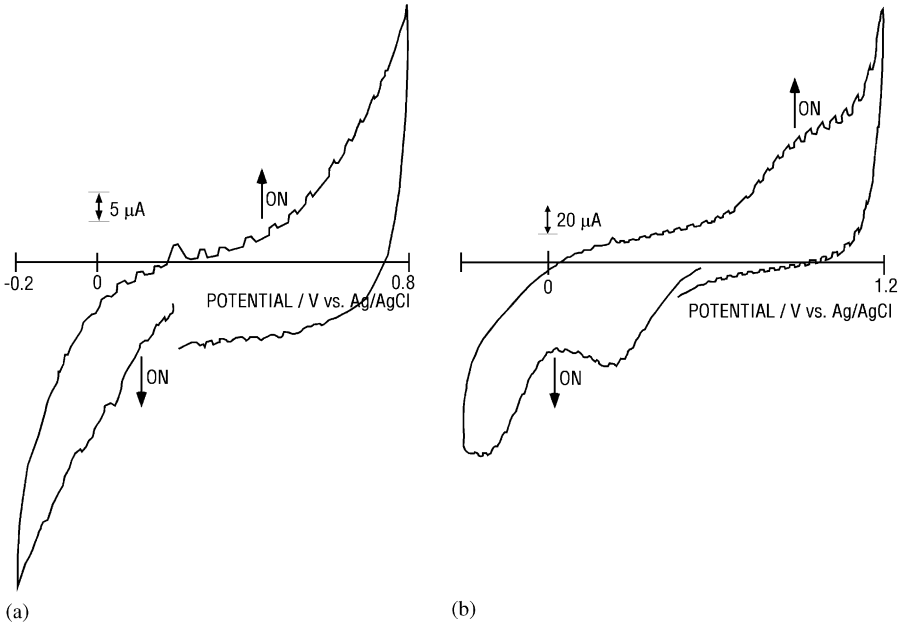

Fig. 7. Cyclic voltammograms of (a) $Ru(bpy)_3^{2+}$ and (b) MB intercalated niobate layered oxide films.

Fig. 8. Electrons produced by the excitation from the HOMO level to the LUMO level of the $Ru(bpy)_3^{2+}$ under the illumination in the visible light range will jump into the conduction band (CB) level of the $[Nb_6O_{17}]^{4-}$ host layer and will move through the band. On the other hand, the produced hole will also move by the tunneling mechanism [14]. Similarly, electron transfer occurs from excited MB* molecules to the $[Nb_6O_{17}]^{4-}$ host layer under visible light illumination. The photoelectrochemical reactions will evaluate H_2 and O_2 gases according to the energy positions.

$Ru(bpy)_3^{2+}$ intercalated niobate layered oxide produced H_2 in the methanol solutions under illumination in the visible light range. The amount of hydrogen evolution is given in Fig. 9. The maximum amount of evolution was reached at 0.28 μmol after 1.5 h. The cessation of the evolution rate might be attributed to the deintercalation of $Ru(bpy)_3^{2+}$ molecules into the methanol solution, because a gradual change in the color of the solution was observed during the experiment. The reaction takes place in the interlayer of the niobate layered oxide. $[Nb_6O_{17}]^{4-}$ host layer gains electrons from the excited $Ru(bpy)_3^{2+}$ molecules in the interlayer and these electrons react with the interlayer H^+ to produce H_2. The result is in agreement with the cyclic voltammogram data in terms of electron transfer mechanism as given above and the mechanism suggested by Furube et al. [33]. No H_2 evolution was observed when the reaction was carried out in pure water. In addition, MB intercalated niobate layered oxide did not produce any H_2 even in methanol–water solution. The inactivity of MB intercalated niobate layered oxide is probably a result of the deintercalation of interlayer MB into the solution soon after the contact. Thus, charge transfer does not occur from deintercalated MB molecules to the host layer. As mentioned previously, interlayer MB molecules are not stable and might deintercalate into the solution easily.

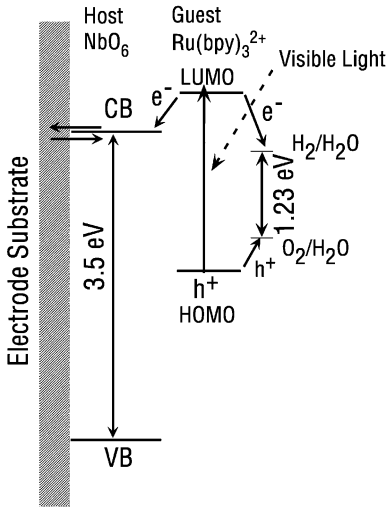

Fig. 8. Possible electron transfer mechanisms for $Ru(bpy)_3^{2+}$ intercalated niobate layered oxides under illumination in the visible light range.

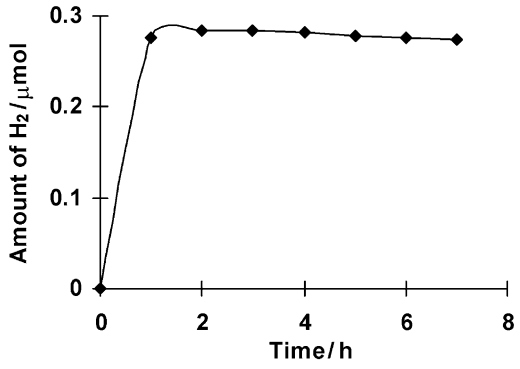

Fig. 9. Photocatalytic H_2 gas evolution on $Ru(bpy)_3^{2+}$ intercalated niobate layered oxide from methanol–water solution under illumination in the visible light range.

4. Conclusion

The intercalation of $Ru(bpy)_3^{2+}$ complex and MB into the interlayer of niobate layered oxides was achieved by ESD method. Individual $[Nb_6O_{17}]^{4-}$ nanosheets exfoliated in TBA solution combine with cations to yield the intercalation compounds. XRD patterns revealed that $Ru(bpy)_3^{2+}$ complex and MB were intercalated into both layers of niobate layered oxide. Co-intercalation of TBA molecules was also observed. Intercalated compound absorbs in the visible light range due to the presence of photoactive molecules that are responsive to visible light in the interlayer. Heat-treatment at 300 °C enhances the interaction between the interlayer $Ru(bpy)_3^{2+}$ complex and host layer, so that electrons formed by excitation from the HOMO level to LUMO level of the complex yields visible light photocurrent. Electron transfer occurs from the excited interlayer molecules to the $[Nb_6O_{17}]^{4-}$ host layer to take part in reactions in the interlayer. $Ru(bpy)_3^{2+}$ intercalated sample was able to produce H_2 in methanol/water system under visible light illumination, but not in pure water.

Acknowledgments

This work was supported by the Core Research for Evolutional Science and Technology (CREST) program of the Japan Science and Technology Co.(JST), and a Grant-in-Aid for Scientific Research (No 15350123) from the Ministry of Education, Culture , Sports, Science, and Technology.

References

[1] N. Kinomura, N. Kumada, F. Muto, J. Chem. Soc. Dalton Trans. 11 (1985) 2349–2351.
[2] R. Abe, J.N. Kondo, M. Hara, K. Domen, Supramol. Sci. 5 (1998) 229–233.
[3] R. Abe, M. Hara, J.N. Kondo, K. Domen, K. Shinohara, A. Tanaka, Chem. Mater. 10 (1998) 1647–1651.

[4] R. Abe, S. Ikeda, J.N. Kondo, M. Hara, K. Domen, Thin Solid Films 156 (1999) 343–344.
[5] L.M. Nunes, A.G. de Souza, R.F. de Farias, J. Alloys Comp. 319 (2001) 94–99.
[6] T. Nakato, Y. Sugahara, K. Kuroda, C. Kato, Mater. Res. Soc. Symp. Proc. 233 (1991) 169–173.
[7] T. Nakato, M. Hirokatsu, K. Kuroda, C. Kato, React. Solids 6 (1988) 231–238.
[8] T. Nakato, D. Sakamoto, K. Kuroda, C. Kato, Bull. Chem. Soc. Jpn. 65 (1992) 322–328.
[9] T. Nakato, K. Kuroda, C. Kato, Catal. Today 16 (1993) 471–478.
[10] M.A. Bizeto, D.L.A. de Faria, V.R.L. Constantino, J. Mater. Sci. 37 (2002) 265–270.
[11] S. Yakabe, T. Nakato, J. Mater. Sci. 38 (2003) 3809–3812.
[12] T. Nakato, H. Miyashita, S. Yakabe, Chem. Lett. 32 (2003) 72–73.
[13] R. Kaito, K. Kuroda, M. Ogawa, J. Phys. Chem. B 107 (2003) 4043–4047.
[14] U. Unal, Y. Matsumoto, N. Tanaka, Y. Kimura, N. Tamoto, J. Phys. Chem. B 107 (2003) 12680–12689.
[15] K. Domen, A. Kudo, M. Shibata, A. Tanaka, K. Maruya, T. Onishi, J. Chem. Soc. Chem. Commun. (1986) 1706–1707.
[16] A. Kudo, A. Tanaka, K. Domen, K. Maruya, K. Aika, T. Onishi, J. Catal. 111 (1988) 67–76.
[17] A. Kudo, K. Sayama, K. Tanaka, K. Asakura, K. Domen, T. Onishi, J. Catal. 120 (1989) 337–352.
[18] K. Sayama, A. Tanaka, K. Domen, K. Maruya, T. Onishi, Catal. Lett. 4 (1990) 217–222.
[19] K. Sayama, A. Tanaka, K. Domen, K. Maruya, T. Onishi, J. Phys. Chem. 95 (1991) 1345–1348.
[20] K. Sayama, K. Yase, H. Arakawa, K. Asakura, A. Tanaka, K. Domen, T. Onishi, J. Photochem. Photobiol. A 114 (1998) 125–135.
[21] R. Abe, K. Shinohara, A. Tanaka, M. Hara, J.N. Kondo, K. Domen, J. Mater. Res. 13 (1998) 861–865.
[22] K. Sayama, A. Tanaka, K. Domen, K. Maruya, T. Onishi, J. Catal. 124 (1990) 541–547.
[23] T. Sato, Y. Yamamoto, Y. Fujishiro, S. Uchida, J. Chem. Soc. Faraday Trans. 92 (1996) 5089–5092.
[24] Y. Fujishiro, S. Uchida, T. Sato, Int. J. Inorg. Mater. 1 (1999) 67–72.
[25] S. Tawkaew, Y. Fujishiro, S. Yin, T. Sato, Colloid. Surf. A 179 (2001) 139–144.
[26] Y.I. Kim, S. Salim, M.J. Huq, T.E. Mallouk, J. Am. Chem. Soc. 113 (1991) 9561–9563.
[27] G.B. Saupe, T.E. Mallouk, W. Kim, R.H. Schmehl, J. Phys. Chem. B 101 (1997) 2508–2513.
[28] Y. Yamaguchi, T. Yui, S. Takagi, T. Shimada, H. Inoue, Chem. Lett. (2001) 644–645.
[29] R. Abe, K. Sayama, H. Arakawa, J. Photochem. Photobiol. A. 166 (2004) 115–122.
[30] T. Nakato, K. Kusunoki, K. Yoshizawa, K. Kuroda, M. Kaneko, J. Phys. Chem. 99 (1995) 17896–17905.
[31] K. Yao, S. Nishimura, T. Ma, K. Okamoto, K. Inoue, E. Abe, H. Tateyama, A. Yamagishi, J. Electroanal. Chem. 510 (2001) 144–148.
[32] K. Yao, S. Nishimura, Y. Imai, H. Wang, T. Ma, E. Abe, H. Tateyama, A. Yamagishi, Langmuir 19 (2003) 321–325.
[33] A. Furube, T. Shiozawa, A. Ishikawa, A. Wada, K. Domen, C. Hirose, J. Phys. Chem. B 106 (2002) 3065–3072.
[34] M. Koinuma, H. Seki, Y. Matsumoto, J. Electroanal. Chem. 531 (2002) 81–85.
[35] G.B. Saupe, C.C. Waraksa, H.K. Kim, Y.J. Han, D.M. Kaschak, D.M. Skinner, T.E. Mallouk, Chem. Mater. 12 (2000) 1556–1562.
[36] K. Domen, Y. Ebina, S. Ikeda, A. Tanaka, J.N. Kondo, K. Maruya, Catal. Today 28 (1996) 167–174.
[37] M.A. Bizeto, V.R.L. Constantino, Mater. Res. Bull. 39 (2004) 1811–1820.
[38] S.H. Bossmann, C. Turro, C. Schnabel, M.R. Pokhrel, L.M. Payawan Jr., B. Baumeister, M. Worner, J. Phys. Chem. B 105 (2001) 5374–5382.
[39] D. Madhavan, K. Pitchumani, Tetrahedron 57 (2001) 8391–8394.